Motion Artifact Cancellation of Seismocardiographic Recording From Moving Subjects

Chenxi Yang, *Member, IEEE*, and Negar Tavassolian, *Member, IEEE*

***Abstract*— This paper presents a novel method of extracting seismocardiographic (SCG) data from moving adult subjects recorded via micro-electromechanical (MEMS) accelerometers. A digital signal processing system based on the normalized least mean square (NLMS) adaptive filter design is developed in MATLAB to process the signals collected from the MEMS sensor node. Standardized experiments were performed on 40 moving adult subjects. False-positives were ruled out for a more precise detection rate. The research on sliding ensemble average was also conducted to find the minimum required window size. The results indicate a detection rate of 96% and a sliding window size of 32 intervals for robust continuous monitoring, showing that adaptive filtering could be a promising technique for the cancellation of motion noise artifacts from SCG recordings in moving subjects.**

***Index Terms*— Adaptive filtering, LMS filtering, MEMS accelerometer, motion artifact, seismocardiography (SCG), wearable sensor network.**

I. Introduction

SEISMOCARDIOGRAM (SCG) is the non-invasive measurements of accelerations on the chest wall produced by myocardial movements of the heart. The clinical aspects of SCG and its advantages over other heart monitoring techniques have been under investigation since the early 1990s [1]. With the development of high-quality, high-sensitivity, and low-cost micro-electromechanical (MEMS) accelerometers in recent years, SCG signals can now be monitored in more robust settings, enabling major breakthroughs in this area [2]. Latest studies mainly focus on wearable sensor healthcare devices, reaching longer monitoring times and providing non-invasive cardiovascular health care [3], [4].

Compared to other heart monitoring methods such as electrocardiogram (ECG), SCG has proven its clinical potential by showing higher sensitivities in detecting coronary artery diseases [5], being a good combinatory sensor for use with electrocardiogram (ECG) electrodes [6], and being compatible with magnetic resonance imaging (MRI) [7]. The SCG signal is representative of the mechanical aspects of the heart while ECG demonstrates its electrical aspects [8], [9]. Modern wireless sensor node solutions for SCG are easy to attach and fast to deploy without any need for skin preparation for electrode attachment. This is a noticeable advantage when applying in emergency monitoring situations.

However, one of the major obstacles for the evolution of SCG towards real-time, continuous, daily healthcare monitoring is the occurrence of motion artifacts (MA) during measurements. If an effective reduction of MA is performed, the applications of SCG will be greatly expanded from steady to dynamic positions [10], for example it will have great potential in preventing heart failure diseases during sports [11] as well as daily mobile health care out of hospital for high-risk patients. Compared to ECG devices which are generally employed in these cases, SCG monitors are easier to attach and have lower cost and power consumptions. They also show the capability to be embedded into smartphones.

Recently, Di Rienzo et al. developed an algorithm that selects movement-free data segments from 24-hour recordings of SCG from ambulant subjects [12]. Their threshold for choosing a proper segment is that the standard deviation of the measurement should be smaller than 4 mg (milli-gravity). Pandia et al. implemented a polynomial smoothing filter to cancel motion artifacts in walking subjects and amplify the peak of the heart sound with the trade-off of distorting the acceleration waveform [13]. This method has successfully improved the heartbeat detection rate but the exact SCG graph from the moving segments could not be recovered.

Our group has recently developed a novel method of recovering SCG signals from acceleration recordings on moving subjects with a higher motion tolerance compared to previous works mentioned above [14]. This paper improves and expands on our previous work in the following areas:

1) The number of subjects under experiments was greatly increased from 11 to 40.

2) Measurements were completely standardized.

3) We ruled out the false-positive detected SCG beats for a more precise evaluation of the detection rate. A study on relationship between MA strength and detection rate was also conducted.

4) In addition to a fixed-point ensemble average analysis, we provided a research on minimum ensemble window size with sliding window along time.

II. Method

A. The Hardware System

Measurements were performed using a commercial wearable wireless sensor node (Shimmer 2, Shimmer Sensing [15])

Manuscript received November 15, 2105; revised February 9, 2016; accepted May 24, 2016. Date of publication May 26, 2016; date of current version June 16, 2016. This paper was presented at the Biomedical Circuits and Systems Conference, Atlanta, GA, USA, October 22–24, 2015. The associate editor coordinating the review of this paper and approving it for publication was Prof. Daniela De Venuto.

The authors are with the Electrical and Computer Engineering Department, Stevens Institute of Technology, Hoboken, NJ 07030 USA (e-mail: cyang13@stevens.edu; negar.tavassolian@stevens.edu).

Digital Object Identifier 10.1109/JSEN.2016.2573269

1558-1748 © 2016 IEEE. Personal use is permitted, but republication/redistribution requires IEEE permission.
See http://www.ieee.org/publications_standards/publications/rights/index.html for more information.

Authorized licensed use limited to: Università di Bari Aldo Moro. Downloaded on October 27,2025 at 23:56:40 UTC from IEEE Xplore. Restrictions apply.

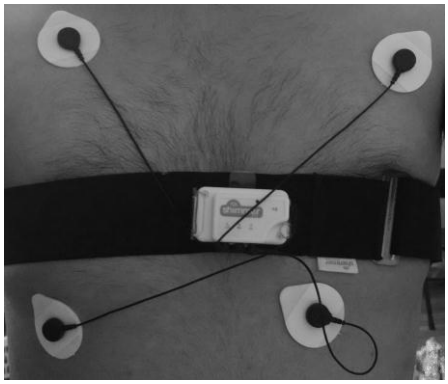

Fig. 1. Measurement setup showing the MEMS accelerometer on the chest strap as well as the four reference ECG electrodes.

with acceleration and ECG measurement capabilities. The sensor was attached on the chest wall of the subjects, placed to the left of the sternum along the third rib using a chest strap as shown in Fig. 1. A pair of lead II (RA-LL) as well as a pair of back-up LA-RL electrodes were connected to the sensor node to record a reference ECG signal simultaneously. A three-axis MEMS accelerometer (MMA 7361, Freescale Semiconductor [16]) captured acceleration data within an acceleration range of ± 1.5 g from the antero-posterior direction, i.e. the z-axis of the sensor where the positive direction was from the chest wall towards the front. Data were collected at a sampling rate of 512 Hz, synchronized, and sent to a computer using Bluetooth.

B. The DSP System

The proposed DSP system diagram is shown in Fig. 2 (a). In our previous work [14], both SCG and ECG signals were low-pass filtered at 50 Hz with a 10^{th}-order finite impulse response (FIR) filter. In this work, we changed the passband frequency for the SCG channel in accordance with a more recent definition of SCG [8] which requires the vibration component to be below 25 Hz, i.e. the infrasonic range. The filtered SCG signal was then fed into the primary channel of a normalized least mean square (NLMS) adaptive filter.

As shown in Fig. 2 (b), the reference channel of the adaptive filter is connected to a delayed version of the primary channel. This structure works as a self-tuning filter which protects narrow-band periodic signals from interference [17], [18]. The delay should be long enough for the broad-band noise to become de-correlated from the primary input signal [17]. The step size for adaptation is tuned to a value of 0.05 in our application. The reason behind applying this method to our specific application was its suitability in cancelling motion segments in single-sensor solutions. In addition, NLMS adaptive filtering has shown great potential for embedding into field-programmable gate arrays (FPGA) [19], [20] or application-specific integrated circuits (ASIC), which provides the potential for specifically-designed hardware developments in the future.

After the motion artifact (MA) cancellation step, peak detection algorithms were applied to both types of signals. The ECG signal was processed with an R-peak detection algorithm

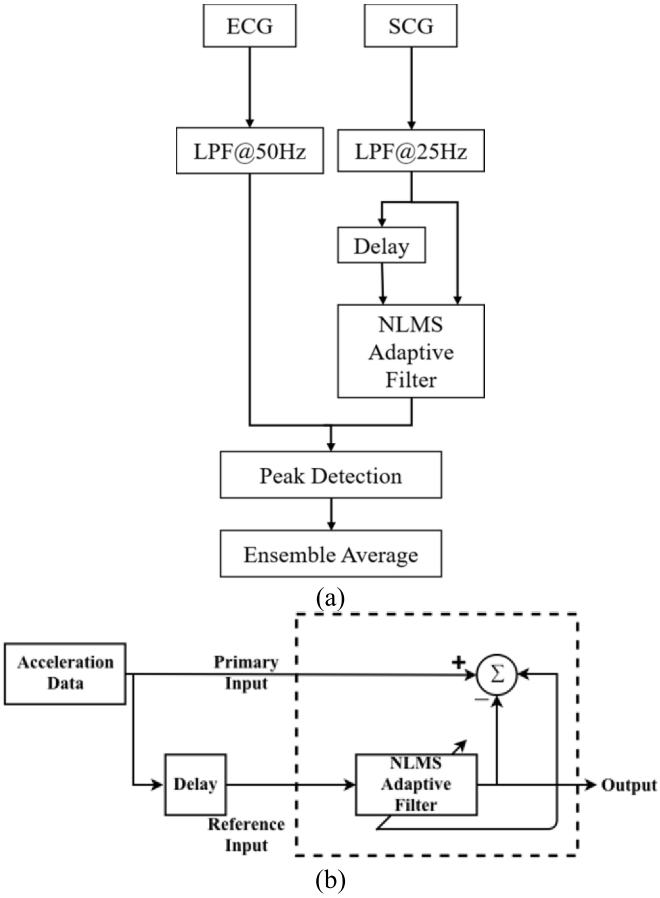

Fig. 2. (a) Block Diagram of the DSP system. (b) Structure of the adaptive NLMS filter.

while the SCG signal was processed with an aortic valve open (AO-peak) detection scheme. Both methods were developed by modifying the idea proposed in [21]. The first step is to search and locate the maxima in the first one-second interval of recordings, i.e. the first 512 samples in the case of our application. The next maxima is then found in the following one-second interval with a delay to avoid the two peaks being too close to each other. In our system, the delay for the ECG signal is 0.2 seconds while the delay for the SCG signal is 0.4 seconds. The cardiac intervals were then segmented using the reference point from the peak detection step.

Although the capability of a beat-to-beat analysis of SCG has been suggested [22], it is not a stable analysis method for moving subjects. We therefore looked into an ensemble-average of the SCG waveform. Since in the previous step the R-peaks and AO-peaks were detected and located, we can calculate the means of the cardiac interval periods by taking the differences between time intervals and then averaging them. The size of the ensemble window was evaluated to search for the minimum window size that would yield a reasonable quality of the SCG graph (all peaks detectable). The results are presented in Section IV.B.

III. Experimental Setup and Protocol

The experiments and analysis were standardized and extensively expanded compared to our previous work.

Authorized licensed use limited to: Università di Bari Aldo Moro. Downloaded on October 27,2025 at 23:56:40 UTC from IEEE Xplore. Restrictions apply.

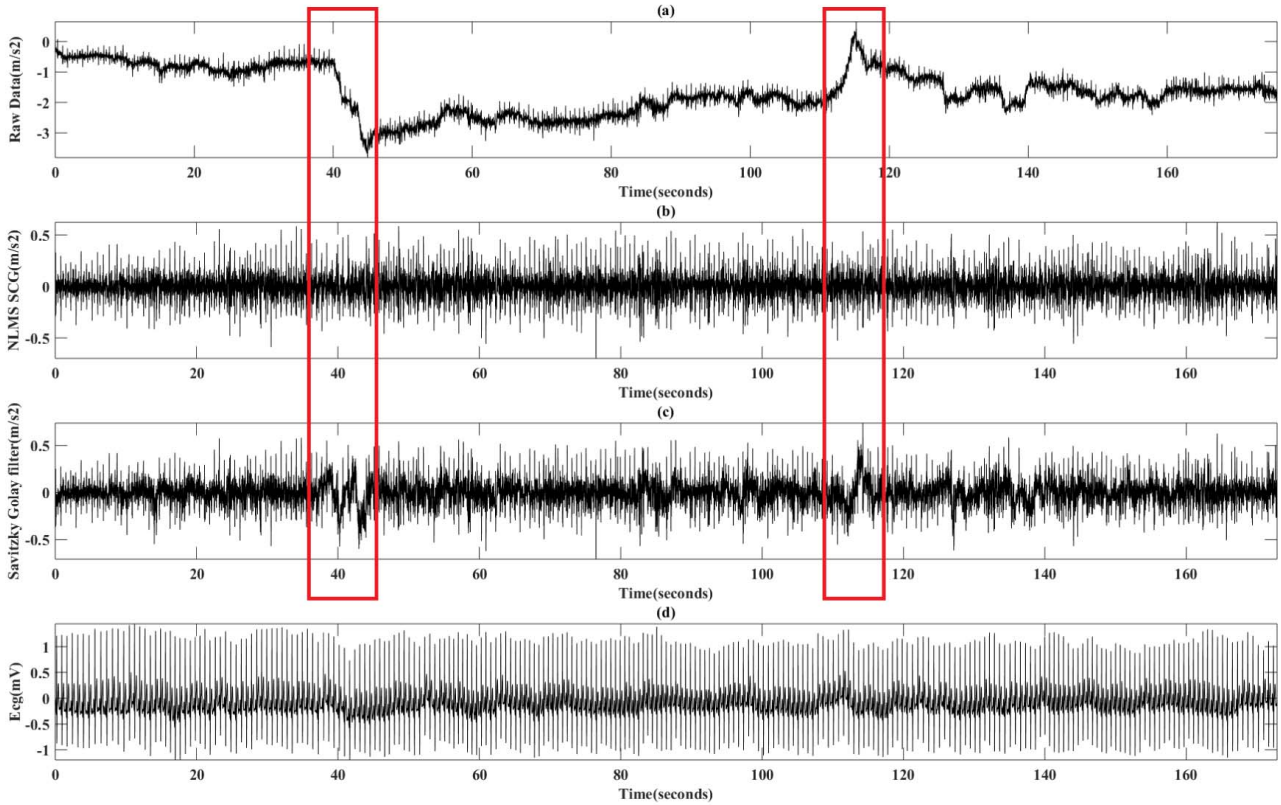

Fig. 3. (a) Raw data from the accelerometer. (b) SCG signal achieved using the proposed method. (c) SCG signal achieved using the polynomial filter proposed in [11]. (d) Reference ECG signal.

TABLE I
HEART RATE DETECTION RATES FROM THE 40 SUBJECTS UNDER STUDY

Subject	SCG Peaks	False-Positives	Detection Rate	Subject	SCG Peaks	False-Positives	Detection Rate
1	193	3	97.93%	**21**	180	4	97.78%
2	200	15	95.36%	**22**	194	5	94.50%
3	205	7	92.09%	**23**	215	3	97.69%
4	204	3	98.05%	**24**	204	3	98.04%
5	207	10	96.10%	**25**	195	2	97.97%
6	192	6	96.88%	**26**	190	4	97.38%
7	193	7	95.38%	**27**	199	5	96.52%
8	199	6	96.50%	**28**	190	5	95.85%
9	178	2	98.88%	**29**	188	3	97.36%
10	196	5	96.95%	**30**	176	5	96.61%
11	181	5	95.65%	**31**	184	4	96.25%
12	186	4	96.80%	**32**	189	3	97.89%
13	188	8	95.74%	**33**	191	6	95.85%
14	196	6	95.47%	**34**	194	4	96.44%
15	189	4	97.36%	**35**	192	7	93.90%
16	190	3	97.39%	**36**	191	5	96.87%
17	197	4	95.07%	**37**	194	6	94.95%
18	210	5	94.03%	**38**	202	4	95.65%
19	209	2	98.57%	**39**	196	3	95.07%
20	188	5	97.86	**40**	196	5	95.5%

Human experiments were approved by the Committee for the Protection of Human Subjects at Stevens Institute of Technology. Forty healthy adult subjects were kept at rest for a period of at least 10 seconds before starting to perform walking movements for 3 minutes. Walking was performed at a speed of less than 1.3 m/s. All measurements were performed

Authorized licensed use limited to: Università di Bari Aldo Moro. Downloaded on October 27,2025 at 23:56:40 UTC from IEEE Xplore. Restrictions apply.

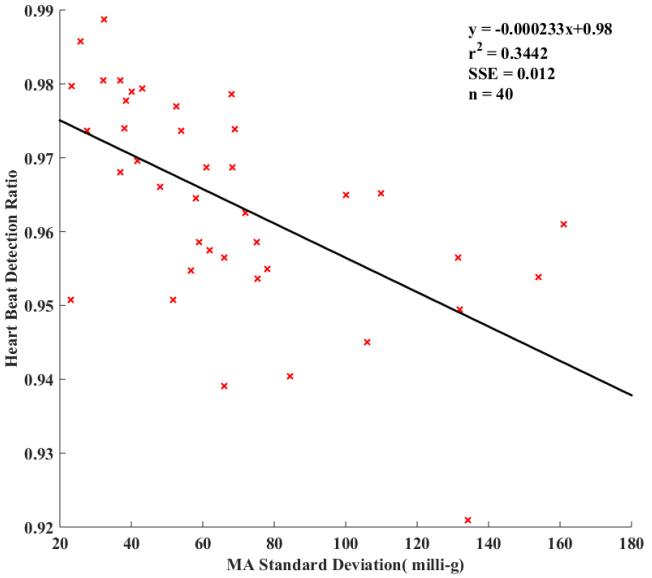

Fig. 4. Correlation analysis between the detection rate and the MA strength.

in a lab environment which is considered as having weak external vibrations.

A fixed length of 90,000 samples (approximately 175 seconds) out of the 3 minutes of recording was evaluated to ensure consistency in signal length and effectiveness of measurement.

IV. Experimental Results

Fig. 3 shows the time-domain plots obtained from a measurement and the subsequent signal processing steps. Fig. 3.a shows the raw acceleration data measured from the sensor. Fig. 3.b illustrates the processed SCG signal, which is achieved after the low-pass filtering and NLMS adaptive filtering steps performed on the acceleration data. For comparison purposes, the result of a Savitzky Golay smoothing filter designed in [13] is demonstrated in Fig. 3.c and the reference ECG signal is plotted in Fig. 3.d. It can be observed that the proposed NLMS adaptive filter outperforms the polynomial smoothing filter. In particular, the adaptive filter shows a clear advantage in the reduction of the motion artifacts during intervals of more extreme movements (marked with red rectangles). From the envelope of this waveform we can still observe MA interference on the amplitude of SCG wave form, and thus an ensemble average analysis will be performed as described in Section IV.B and its effect will be evaluated.

The employed metrics for analyzing the data are explained below.

A. Detection Rate With False Positives and MA Strength Analysis

Table I illustrates the heart beat detection rate defined as the number of detected SCG beats over ECG beats observed during the same time interval. The false-positive detected SCG beats were also considered and ruled out to give a more precise estimate of detection rate. In addition, the standard deviation (std. dev.) of acceleration was calculated in order

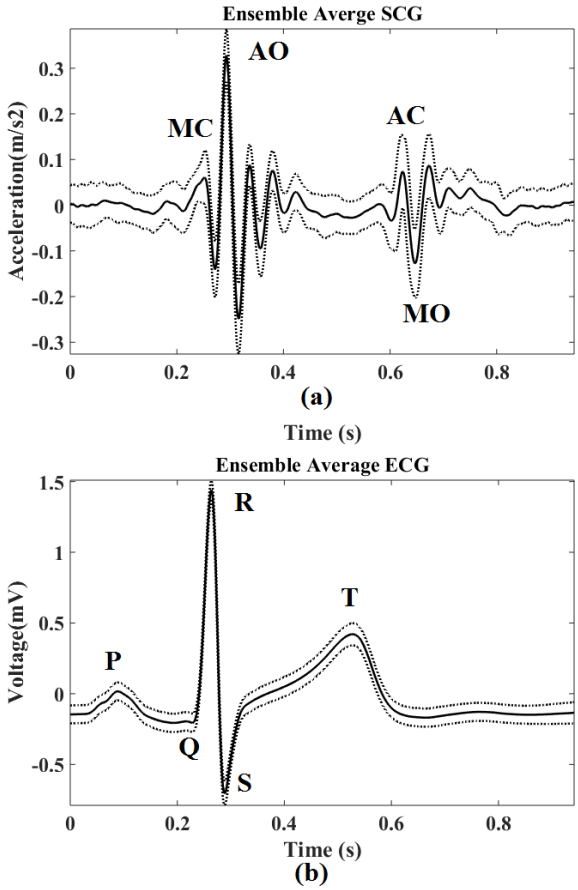

Fig. 5. Ensemble averages of (a) SCG and (b) ECG signals over 204 intervals.

to evaluate the relationship between the system performances, i.e. true detection rate, and MA strength.

Experimental evaluations from 40 healthy subjects reveal a false-positive detection peak of 4.9 numbers in average with std. dev. of 2.362. After ruling out the false-positive peaks, the detection rate has an average of 96.40% with a std. dev. of 1.42%. The correlation coefficient between MA strength and detection rate is -0.586. Fig. 4 demonstrates the correlation analysis between the MA strength and detection rate. Although a negative linear relationship between these two factors is revealed as expected, the R-squared value is relatively low, indicating that the MA strength is not the sole factor interfering with the detection rate. Some other probable factors are expected be weight, BMI, and walking posture.

It is seen that a detection rate of above 98% will be achieved if the MA strength is between 20 and 40 mg in std. dev. Compared to the threshold of [12] which is 4 mg, our proposed system shows significant improvements in the tolerance of MI and suggests possible detection of all useful heartbeat peaks during movement of the subject.

B. SCG Recovery With a Sliding Window Along Time

Fig. 5 illustrates the ensemble average recovery plots of the SCG and reference ECG signals from a subject over 204 intervals (detection rate: 98.05%, MA strength: 32.1 mg in std. dev.). The AO and R peaks are automatically picked for

Authorized licensed use limited to: Università di Bari Aldo Moro. Downloaded on October 27,2025 at 23:56:40 UTC from IEEE Xplore. Restrictions apply.

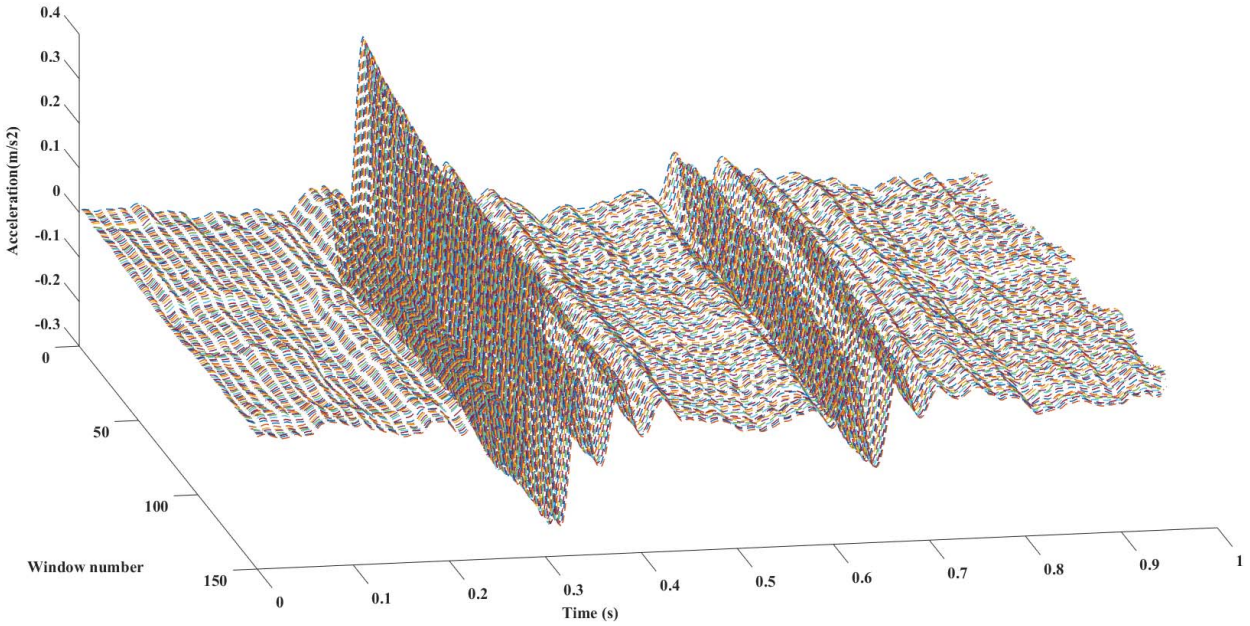

Fig. 6. Ensemble average SCG with 32 sliding interval windows along time.

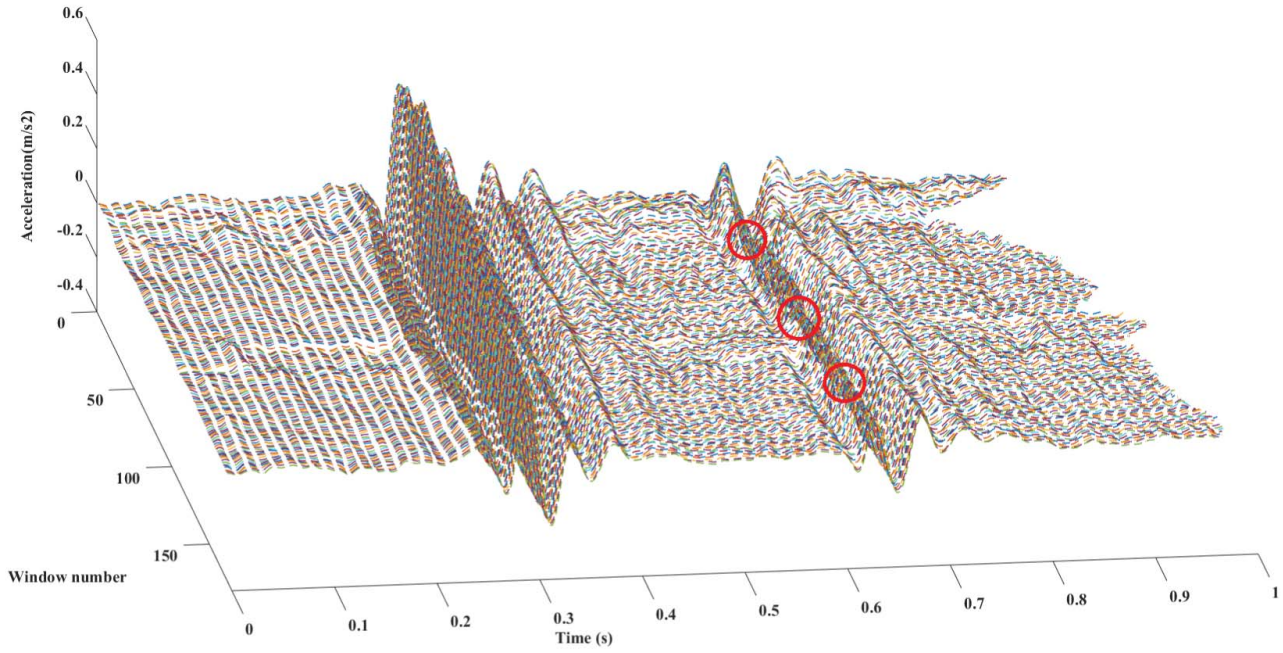

Fig. 7. Ensemble average SCG with window size of 16, showing 3 missing AC-peaks.

the ensemble window selects. Other peaks are then manually interpreted on the ensemble-average graphs. The mitral valve closure-aortic valve open (MC-AO) peak in the SCG signal and the QRS complex in the ECG signal are clearly demonstrated. Aortic valve closure (AC) and mitral valve opening (MO) of the SCG signal can also be detected as they occur after the T-wave in the ECG signal.

The ensemble window size is a critical parameter that reflects the potential of the proposed system for real-time performance. Our previous investigation had suggested that a window size of 16 intervals might be sufficient for satisfactory detection under all situations. As MA may vary along time during a measurement, we applied an improved sliding window ensemble average evaluation on each subject to observe the overall performance. The results indicated that 16 is not a stable window size for all conditions as it shows missing peaks in some samples. Fig. 6 and 7 illustrate the sliding window ensemble average over time in 3-D representations. Time of each ensemble average is shown along the x-axis and sliding windows are distributed along the y-axis. The z-axis

Authorized licensed use limited to: Università di Bari Aldo Moro. Downloaded on October 27,2025 at 23:56:40 UTC from IEEE Xplore. Restrictions apply.

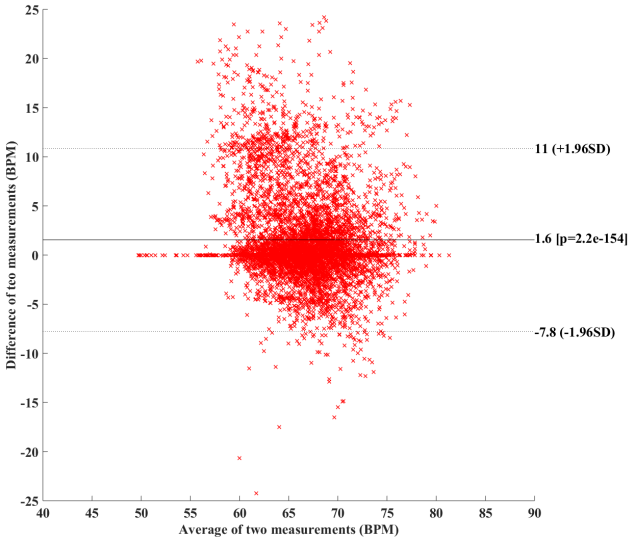

Fig. 8. Bland-Altman plot between SCG and ECG heart rate measurements.

shows the amplitudes of each ensemble average graph. Fig. 6 depicts a stable sample with window size of 32 in which all the peaks have been detected while Fig. 7 shows a sample with 3 missing AC-peaks out of 188 peaks when window size of 16 was used. No quality loss was observed at ensemble size of 32. This result indicates that with a trade-off of 32 cardiac interval delay, it would be possible to track heart activity continuously on ambulant subjects.

C. Bland-Altman Analysis

To further analyze the agreement between AO-AO and R-R intervals, a Bland-Altman plot is generated and illustrated in Fig. 8. The average of the SCG and ECG heart rate measurements is marked on the x-axis while their difference is shown on the y-axis. Heart rate is calculated from the sliding average of 5 cardiac intervals with its unit in beats per minute (BPM). It is observed that most measurements lie in the 95% confidence region. The outliners are believed to be resulting from extreme movements of the subjects.

V. Discussion and Conclusions

This paper presents the results of a novel method proposed for motion artifact cancellation of SCG recordings in moving subjects. Experimental results from standardized experiments indicate the feasibility of tracking SCG signals during subject movement. System tolerance on MA is below 40 mg for a detection rate more than 98%. Sliding ensemble average window size of 32 has been suggested for robust and continuous operation of the system.

From the hardware point of view, a mobile wearable device should have low power consumption, and therefore optimizations on wireless transmission and signal pre-processing methods need to be performed. A proper compressing before streaming or storing data would greatly reduce the power consumption of the system. Some algorithms such as compressed sensing [23] have been tested on ECG signals and have shown great potential for implementation on SCG as well.

In order to provide a better analysis on the factors that influence detection rate, more demographic information should be collected from each subject including weight, gender, and BMI. More advanced algorithms should be tested based on our framework to cancel larger levels of MA and achieve a smaller sliding window size. Improvements in the peak or interval detection would push this research towards higher detection rates and more robustness, closing the gap between research and real-life applications.

References

[1] D. M. Salerno and J. Zanetti, "Seismocardiography for monitoring changes in left ventricular function during ischemia," *CHEST J.*, vol. 100, no. 4, pp. 991–993, 1991.

[2] O. T. Inan *et al.*, "Ballistocardiography and seismocardiography: A review of recent advances," *IEEE J. Biomed. Health Inform.*, vol. 19, no. 4, pp. 1414–1427, Jul. 2014.

[3] M. Di Rienzo *et al.*, "A wearable system for the seismocardiogram assessment in daily life conditions," in *Proc. IEEE Annu. Int. Conf. Eng. Med. Biol. Soc.*, Aug./Sep. 2011, pp. 4263–4266.

[4] K. Tavakolian, "Characterization and analysis of seismocardiogram for estimation of hemodynamic parameters," Ph.D. dissertation, School Eng. Sci., Simon Fraser Univ., Burnaby, BC, Canada, 2010.

[5] R. A. Wilson, V. S. Bamrah, J. Lindsay, Jr., M. Schwaiger, and J. Morganroth, "Diagnostic accuracy of seismocardiography compared with electrocardiography for the anatomic and physiologic diagnosis of coronary artery disease during exercise testing," *Amer. J. Cardiol.*, vol. 71, no. 7, pp. 536–545, 1993.

[6] D. M. Salerno, J. M. Zanetti, L. A. Green, M. R. Mooney, J. D. Madison, and R. A. Van Tassel, "Seismocardiographic changes associated with obstruction of coronary blood flow during balloon angioplasty," *Amer. J. Cardiol.*, vol. 68, no. 2, pp. 201–207, Jul. 1991.

[7] M. Jerosch-Herold *et al.*, "The seismocardiogram as magnetic-field-compatible alternative to the electrocardiogram for cardiac stress monitoring," *Int. J. Cardiac Imag.*, vol. 15, no. 6, pp. 523–531, Dec. 1999.

[8] J. M. Zanetti and K. Tavakolian, "Seismocardiography: Past, present and future," in *Proc. 35th Annu. Int. Conf. IEEE Eng. Med. Biol. Soc. (EMBC)*, Jul. 2013, pp. 7004–7007.

[9] O. Postolache, P. Girão, and G. Postolache, "Seismocardiogram and ballistocardiogram sensing," in *Advanced Instrument Engineering: Measurement, Calibration, and Design*. Hershey, PA, USA: IGI Global, 2013, p. 223.

[10] L. G. Futterman and R. Myerburg, "Sudden death in athletes," *Sports Med.*, vol. 26, no. 5, pp. 335–350, Nov. 1998, doi: 10.2165/00007256-199826050-00004.

[11] J. P. Neary, D. S. Macquarrie, V. Jamnik, N. Gledhill, S. Gledhill, and E. F. G. Busse, "Assessment of mechanical cardiac function in elite athletes," *Open Sports Med. J.*, vol. 5, pp. 26–37, 2011.

[12] M. Di Rienzo, P. Meriggi, E. Vaini, P. Castiglioni, and F. Rizzo, "24 h seismocardiogram monitoring in ambulant subjects," in *Proc. IEEE Eng. Med. Biol. Soc. (EMBC)*, Aug./Sep. 2012, pp. 5050–5053.

[13] K. Pandia, S. Ravindran, R. Cole, G. Kovacs, and L. Giovangrandi, "Motion artifact cancellation to obtain heart sounds from a single chest-worn accelerometer," in *Proc. IEEE ICASSP*, Dallas, TX, USA, Mar. 2010, pp. 590–593.

[14] C. Yang and N. Tavassolian, "Motion noise cancellation in seismocardiographic monitoring of moving subjects," in *Proc. IEEE Biomed. Circuits Syst. Conf. (BioCAS)*, Oct. 2015, pp. 1–4.

[15] (2016). *Shimmer Sensing*. [Online]. Available: http://www.shimmesensing.com/

[16] Freescale Semiconductor. *±1.5 g, ±6 g Three Axis Low-g Micromachined Mccelerometer*. [Online]. Available: http://www.freescale.com/files/sensors/doc/data_sheet/MMA7361L.pdf

[17] B. Widrow *et al.*, "Adaptive noise cancelling: Principles and applications," *Proc. IEEE*, vol. 63, no. 12, pp. 1692–1716, Dec. 1975.

[18] S. O. Haykin, *Adaptive Filter Theory*. Englewood Cliffs, NJ, USA: Prentice-Hall, 2002.

[19] D. T. M. Slock, "On the convergence behavior of the LMS and the normalized LMS algorithms," *IEEE Trans. Signal Process.*, vol. 41, no. 9, pp. 2811–2825, Sep. 1993.

[20] I. Homana, I. Muresan, M. Topa, and C. Contan, "FPGA implementation of LMS and NLMS adaptive filters for acoustic echo cancellation," *ACTA Technica Napocensis-Electron. Telecommun.*, vol. 52, no. 4, pp. 13–16, 2011.

Authorized licensed use limited to: Università di Bari Aldo Moro. Downloaded on October 27,2025 at 23:56:40 UTC from IEEE Xplore. Restrictions apply.

[21] K. H. Parker, *A Practical Guide to Wave Intensity Analysis*. [Online]. Available: http://www.bg.ic.ac.uk/research/k.parker/guide_to_wia/00_introduction.html
[22] M. J. Tadi, E. Lehtonen, T. Koivisto, M. Pänkäälä, A. Paasio, and M. Teräs, "Seismocardiography: Toward heart rate variability (HRV) estimation," in *Proc. IEEE Int. Symp. Med. Meas. Appl. (MeMeA)*, May 2015, pp. 261–266, doi: 10.1109/MeMeA.2015.7145210.
[23] H. Mamaghanian, N. Khaled, D. Atienza, and P. Vandergheynst, "Compressed sensing for real-time energy-efficient ECG compression on wireless body sensor nodes," *IEEE Trans. Biomed. Eng.*, vol. 58, no. 9, pp. 2456–2466, Sep. 2011.

Chenxi Yang (M'13) received the B.Eng. degree in measuring control technology and instruments from Southeast University, Nanjing, China, in 2013, and the M.Eng. degree in electrical engineering from the Stevens Institute of Technology, Hoboken, NJ, in 2015, where he is currently pursuing the Ph.D. degree in electrical engineering. His research interests are biophysical signal processing and mobile healthcare with sensor networks. He is a student Member of the IEEE Signal Processing Society. He received the Conference Travel Award for his paper at the IEEE BIOCAS 2015, Atlanta, GA.

Negar Tavassolian received the B.Sc. degree from the Sharif University of Technology, Tehran, Iran, in 2003, the M.Sc. degree from McGill University, Montreal, QC, Canada, in 2006, and the Ph.D. degree from the Georgia Institute of Technology, Atlanta, GA, in 2011, all in electrical engineering. She was a Post-Doctoral Fellow with the David H. Koch Institute for Integrative Cancer Research, Cambridge, MA, from 2011 to 2013. She has been an Assistant Professor with the Stevens Institute of Technology, Hoboken, NJ, USA, since 2013. Her main research interests are non-invasive diagnostic methods, nuclear magnetic resonance-based sensors and systems, bio and applied electromagnetics, and microelectromechanical systems.

Authorized licensed use limited to: Università di Bari Aldo Moro. Downloaded on October 27,2025 at 23:56:40 UTC from IEEE Xplore. Restrictions apply.